App. Envi. Res. 43(3) (2021): 45-59

Applied Environmental Research

Journal homepage : http://www.tci-thaijo.org/index.php/aer

Flood Hazard Mapping and Assessment of Precipitation Monitoring System Using GIS-Based Morphometric Analysis and TRMM Data: A Case Study of the Wadi Qena Watershed, Egypt

Wael M. Elsadek[1,*], Wael Elham Mahmod[2,3], Mona G. Ibrahim[4,5]

[1] Civil Engineering Department, Faculty of Engineering, South Valley University, Qena, Egypt
[2] Civil Engineering Department, Faculty of Engineering, Assiut University, Assiut, Egypt
[3] Civil Engineering Department, Faculty of Engineering, Taif University, Taif, Kingdom of Saudi Arabia
[4] Dean of School of Energy Resources, Environment, Chemical and Petrochemical Engineering, Egypt-Japan University of Science and Technology
[5] Environmental Health Department, High Institute of Public Health, Alexandria University, Egypt
[*] Corresponding author: Wael.Elsadek@ejust.edu.eg

Article History
Submitted: 16 September 2020/ Revision received: 30 December 2020/ Accepted: 22 January 2021/ Published online: 22 July 2021

Abstract

Wadi Qena is one of the Nile Valley areas particularly at risk of severe flash flooding, located in Egypt. The study aims to verify TRMM rainfall data (TRMM 3B42), using eight stations across Egypt as well as relies on morphometric analysis to generate a flood risk map based on the ranking method. Three process could be recognized through the study, calibration, correction and verification processes. The results discuss the match daily rainfall trends of TRMM and observed data, producing a correction equation for TRMM data with root mean square error (RMSE) value of 0.837 mm d^{-1} and R^2= 0.238 (calibration process). On the other hand, a verification process, using the developed correction equation, obtain RMSE value of 1.701 mm d^{-1} and R^2= 0.601. The morphometric analysis shows 32 sub-basins with a hazard degree from moderate to high, amounting to 50.3% of the watershed area. Conclusively, this study confirms that the current monitoring system is not enough to cover the whole area, especially the high-risk sub-basins, and TRMM data could provide key information for water-related applications in Egypt.

Keywords: TRMM data; Flood hazard; Morphometric parameters; Wadi Qena; Monitoring system

Introduction

In a broad sense, disasters are defined as dangerous events that may lead to injury or loss of life, with or without property loss. Disasters affect society in terms of the physical, social and economic losses and because human activities are interrupted as a result [1]. Flash floods are

https://doi.org/10.35762/AER.2021.43.3.4

considered a hazard that can lead to catastrophic outcomes in arid, mountainous areas, threatening life and property, and damaging infrastructure. Damage from flash floods increases in severity in areas where infrastructure is incompetent, and warning systems are insufficient or missing [2] because the warning systems give the chance for taking the necessary precautions. Moreover, flash floods in arid regions are characterized by rapid formation [3] where there are no buildings or land cover that represent flood obstacles to form rapidly as they are in urban areas. Furthermore, floods can bring pathogens into urban environments, and cause lingering damp and microbial development in buildings and infrastructure [4]. Heavy rains are the main mechanism, and the primary component of flash floods [5]. The measured data of rainfall from ground stations are associated with certain failings due to data transfer problems during flood events and/or post-flood maintenance requirements [6]. Despite the problem as mentioned above facing ground-based rain measurement systems, remote sensing precipitation products, especially satellite precipitation estimates, are relatively free of these problems.

The success of TRMM in hydrology has led to serious discussions about the use of the space observations system to monitor precipitation, soil moisture, and surface discharge for operational flood warnings [7]. Furthermore, Borga et al. [8] claim that flood system's main component is the rainfall detection by remote sensing and numerical weather forecasts. Moreover, Almazroui [9] asserts that TRMM results are good enough to be used in a variety of water-related applications over the Kingdom of Saudi Arabia. Kheimi and Gutub [10] evaluated the performance of various satellite rainfall estimator products (TRMM 3B42, CMORPH, GSMaP_MVK and PERSIANN) around Saudi Arabia, with a spatial resolution of 0.25° for TRMM 3B42, CMORPH and PERSIANN, and 0.1° for GSMaP_MVK, concluding that TRMM 3B42 offers the best possibility for accurate estimation and variability of precipitation with such high spatial resolution. The three-hourly 3B42RT images covering the 2000–2013 period were used for flash flood forecasting. It was the first time that 3B42RT data have been used for flood monitoring purposes, and the 3B42RT detected high-intensity rainfall events matched to the observed flood distribution over the Kingdom of Saudi Arabia [11].

On the other hand, morphometric analysis plays an effective role in flood risk detection. Accordingly, Saleh [12] determined factors that influence flash flood severity, such as drainage networks, drainage orders, and drainage characteristics. Analysis of the morphometrical parameters of drainage basins is also required to minimize the effects of flash floods [13]. Moreover, Bajabaa et al. [14] studied quantitative analysis of morphometric parameters, such as basin area, perimeter, stream frequency, drainage density, ruggedness number, and texture ratio. Moreover, quantitative techniques have been applied to study the morphometric properties of different drainage basins in India, such as the Morar River Basin and Madhya Pradesh [15]. Geographic information systems (GIS) and remote sensing (RS) are useful tools in disaster management for watersheds. The application of GIS to examine morphometric and geological features of gypsum karst in the Sivas Basin was described by Keskin and Yılmaz [16]. Sanyal and Lu [17] and Zerger [18] have also presented a review of remote sensing and GIS in flood susceptibility mapping in Asia's developing countries and in various case studies, such as India and Cairns, located in far northern Australia. Sharma et al. [19] used GIS technique for performing the analysis of quantitative morphometric in eight sub-basins of the Uttala River sub-watershed in India. The results showed that two sub-basins were subject to relatively higher erosion and soil losses, and suitable soil erosion control measures were

required in these sub-watersheds to preserve the land from further erosion. Zope et al. [20] used GIS and remote sensing data to study the impact of land use and land cover on flood hydrographs for different return periods, using the HEC-GeoHMS and HECHMS models.

In Egypt, flash floods frequently occur in many regions, namely Upper Egypt, the Eastern Desert of Egypt, and the Sinai Peninsula. Morphometric analysis and prioritization of watersheds are very important for water resource modelling and flood management [21]. Elewa et al. [22] have also introduced a detailed hydro-morphometric analysis for the El-Arish watershed in the north and central Sinai to highlight the priority areas for runoff water harvesting (RWH) which means concentration, collection, storage and use of rainwater by runoff for various purposes such as domestic, animal and agricultural use. Moawad et al. [23] and Elsadek et al. [24–26] argue that given its history of flash floods, Wadi Qena should be considered a high-risk area in the Nile Valley in terms of flooding and economic losses and assess the susceptibility of Wadi Qina watershed sub-catchments based on morphological parameters. The potential damage due to flash floods in Wadi Qena involves cutting off main roads, breaking water pipelines, and lossing lives. The problems related to flooding have increased due to quick human activitys' growth, making it necessary to recognize flood-prone areas.

Unfortunately, the quantity and quality of data available for analysis of flooding in Wadi Qena are generally very poor, with specific weaknesses as follows:

• Geographic topography planning is largely planimetric in content and topographic data are based primarily on the Shuttle Radar Topography Mission with the 90-m resolution at ground level;

• No records are obtainable regarding flood frequency or flow rise. If records are existing, they are insufficient, often narrative, and not supported by evidence.

• The study area suffers from a scarcity of recorded rainfall data, which is the main partner (together with morphometric parameters) in flood assessment.

The aim of this work is to calibrate TRMM rainfall data with reference to the available observed data. Moreover, monitor the changes in the seasonal and regional climate in dry regions, such as Wadi Qena, after investigating satellite data availability where traditional measurement instruments are sparse. A flood hazard map is to be constructed to estimate the flood risk levels of the sub-watersheds within Wadi Qena and to assess the current monitoring system (gauge measurements).

Study area

Wadi Qena is considered one of the biggest valleys in the Eastern Desert situated in upper Egypt on the east bank of Qena meander. Wadi Qena has mountainous crests running parallel to the Red Sea coast, but the River Nile is situated on the western side. The mountainous area which located on the eastern boundary varies in elevation by ranges from 77 m to 1866 m above the mean sea level (AMSL) as illustrated in Supplementary Material (SM) 1. Qena city is 608 km away from Cairo, which is the Wadi Qena outlet, as shown in Figure 1a. Various activities are associated with the study area, including tourism, gold mining, and military bases. The importance of the study area, based on the New Urban Communities Authority in Egypt, is that it contains the New Qena City project, located within the downstream boundary of Wadi Qena (at the cost of approximately 2,100 million pounds). Figure 1b shows the main road network between the Qena and Sohag governorates on the Nile River and Hurghada city on the Red Sea. These roads are considered the only link between the main cities in the region.

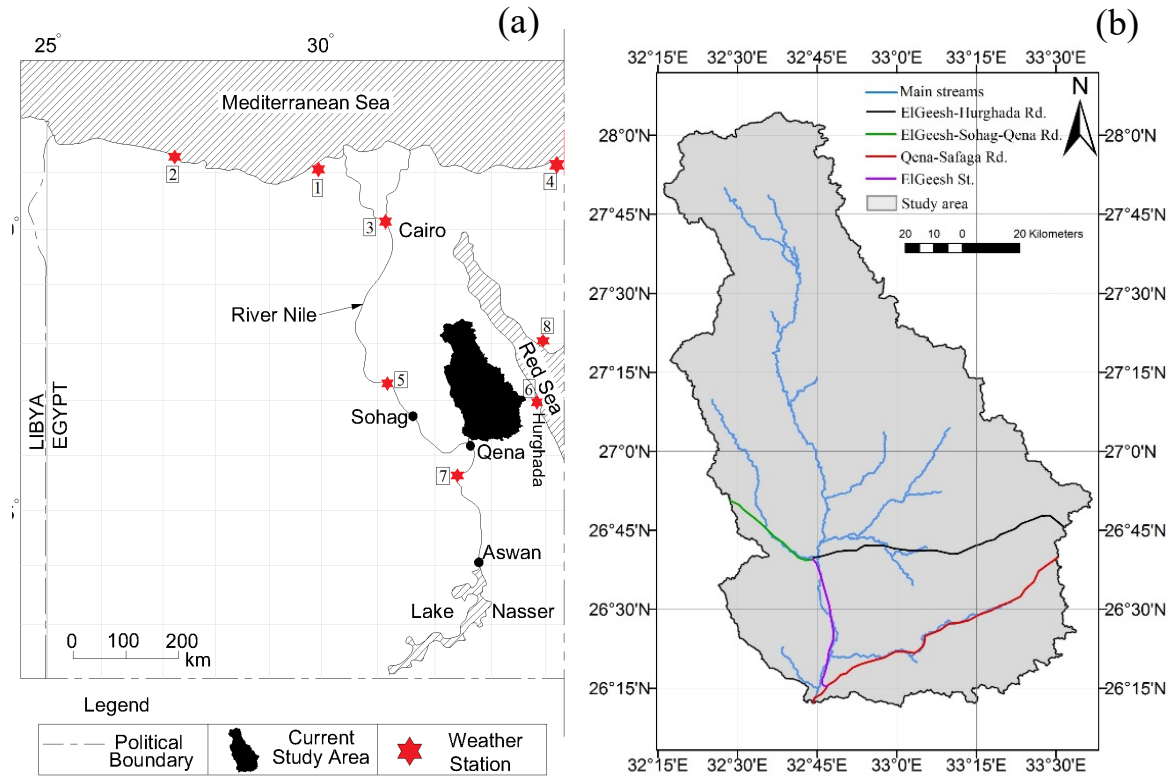

Figure 1 Map of Egypt and the study area location showing: a) location of both study areas and weather stations; b) main roads.

Wadi Qena has a hot desert climate (BWh) according to Köppen climate classification [27] with very hot summers and days in winter feel warm, but cold at night. July and August are the hottest months, while the coldest month is January [23] as shown in SM 2. Geologically, Wadi Qena is characterized by the diversity of its geological structure and rock units, from the pre-Cambrian basement of igneous and metamorphic rocks to Quaternary. The most important are those from Lower Carboniferous/Upper Cretaceous to Eocene, associated with the movement of seawater cycles before the closure of the Tethys [28].

Materials and method

1) Materials

ArcGIS 10.4.2 has been used to create a basis to acquire a deeper understanding of the study area and its drainage system. Terrain analysis is done based on the digital elevation model (DEM), which is obtained from the Shuttle Radar Topography Mission (SRTM) data with a resolution of 90 meters at ground level. DEM is used for analysis of topography and modelling of surface processes, identifying flood risk zones, and is considered the primary component in hydrological models. Terrain analysis involved some processes to get the watershed delineation. These processes are clipping the boundary of the watershed to extract the drainage network of the study area in addition to create flow direction raster. After that, the flow accumulation could be created to get the watershed basin. TRMM used to obtain the satellite-based precipitation data for this study, is a joint project launched by NASA and the Japanese space agency, JAXA. Moreover, TRMM has yielded a range of products created with various processing algorithms. The version used in this study is 3B42 V7, which has a spatial resolution of 0.25° and spans the area between latitudes 50° S and 50° N.

The locations of rain gauges (red asterisks) present in Figure 1a. The study's time series spans 2012 to 2016, a period where there are no missing data for the selected temporal resolution.

2) Method

The methodology separates two phases, data preparation, and data analysis, as shown in Figure 2. The data preparation phase for the rainfall started with the acquisition raw data (TRMM), followed by the calibration process to obtain corrected TRMM data. Meanwhile, the data preparation phase was carried out for the morphometric analysis, beginning with study DEM area, then applying image correction, such as filling the gaps of the DEM images can form. This is done through neighborhood coefficients, which recognize similar neighboring values of pixels. The data analysis step for the rainfall involves analysis of the corrected TRMM data to study temporal and spatial variation of the rainfall over the study area, and assess the monitoring system. The morphometric data analysis involves applying the ranking method to various parameters to generate a flood risk map.

Rainfall data obtained from the TRMM closest to the station (located in a grid box) are compared with the rain gauge's corresponding data. The TRMM Algorithm's performance is characterized by three main categories [29]: underestimation, overestimation and approximation (within ± 10%). Comparing the TRMM day-to-day rainfall with the rain-gauge data is carried out to understand the TRMM performance over the country. The calibration process for the TRMM data involves numerous steps as follows:

- Determining the rainy days observed by the rain gauge, recorded at eight stations across the country (see Figure 1a);
- Calculating the average rainfall from each of the eight stations for each rainy day between 2012 and 2016 (the rainfall data for this period time are complete, with no gaps);
- Calculating the average of the TRMM data for the weather stations over the same period time;
- Dividing the observed data set into two groups, the first of which is plotted against the original TRMM data for calibration and to obtain the correction equation for the TRMM;

The second group of recorded data is plotted against the corrected TRMM data to verify the results and the correction equation.

3) TRMM data calibration

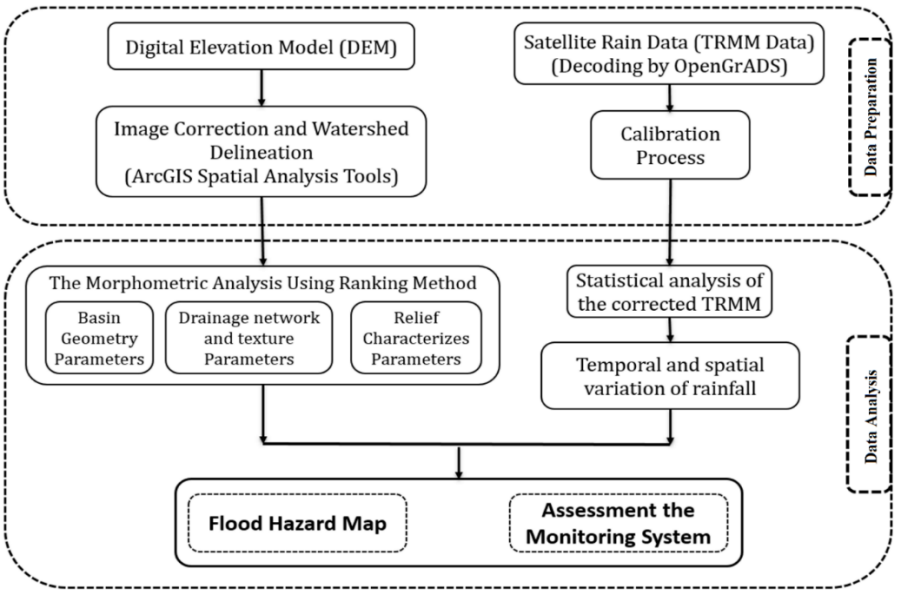

Figure 2 Flowchart of the methodology.

For the study area, analysis of the corrected TRMM data is carried out to study its temporal variation to define the rainy seasons. Four seasons are defined as follows: winter is December to February; spring is March to May; summer is June to August; and autumn is September to November, where three-month averages for meteorological parameters, such as temperature and rainfall, are used to define the seasonal climate according to the American Meteorological Society. The corrected TRMM data are then spatially interpolated using the Kriging method (integrated with GIS) to prepare the rainfall contour maps. Interpolation is carried out using the Kriging method because of its simplicity and ease of use [30].

4) Morphometric analysis

The morphometric analysis is including two parts (as shown in Figure 2), firstly, data preparation using digital elevation model (DEM) and satellite rain data (TRMM), secondly data analysis using ranking method and statistical analysis of the corrected TRMM. The morphometric parameters are applied to derive the morphometric analysis using the ranking method, listed in Table 1, divided into three categories: geometry of the basin, drainage network and texture, and relief characteristics.

For the geometry of the basin, the essential parameters are basin area (A), basin length (Lb), and basin perimeter (Pr). The other parameters, such as basin shape index (Ish), elongation ratio (Re), and compactness ratio (Cc), can be derived based on the relationships between these main parameters (A, Lb and Pr). The parameters (A) and (Ish) are directly proportional to the degree of risk, where the higher the parameter value, the higher is the degree of risk [31–32]. Meanwhile, (Cc) is inversely proportional to the degree of risk, where a low basin value is the most hazardous from a drainage standpoint because of the short time it will take before the occurrence of peak flow in the basin [33].

Table 1 Morphometric parameters

	Morphometric parameters	Formula or method	Reference
Basin geometry	Watershed area (A) (km^2)	ArcGIS software	[35]
	The basin length (Lb) (km)	ArcGIS software	[35]
	The basin perimeter (Pr) (km)	ArcGIS software	[35]
	Elongation ratio (Re)	Re =$(2\sqrt{A/\pi})/Lb$	[35]
	Basin shape index (Ish)	Ish = $\frac{1.27\ A}{LB\text{^}2}$	[36]
	Compactness ratio (Cc)	SH = $\frac{Pr}{2\sqrt{\pi A}}$	[33]
Drainage network and texture	Stream Order (u)	ArcGIS software using Hierarchical rank	[33],
	Stream number (Nu)	Nu= N1+N2+N3+……+Nn	[37–38]
	Stream length (Lu)	Lu= L1+L2+L3+…….+Ln	[37]
	Texture ratio (Rt) (km^{-1})	Rt = $\frac{\sum Nu}{Pr}$	[33]
	Stream frequency (F)	$\boldsymbol{F = \frac{\sum Nu}{A}}$	[39]
	Drainage density (D) (km^{-1})	$\boldsymbol{D = \frac{\sum Lu}{A}}$	[33, 39]
Relief characterizes	Mean basin slope (Sm)	GIS	
	Maximum elevation (Hmax) (m)	GIS	
	Minimum elevation (Hmin) (m)	GIS	
	Relief (Rf) (m)	Rf = Hmax – Hmin	
	Relief Ratio (Rr)	Rr = Rf / Lb	[37]
	Ruggedness number (Rn)	Rn= Rf*D	[35]

The parameters texture ratio (Rt), stream frequency (F), and drainage density (D) in the category of the drainage network and texture can be calculated using the relationships between the stream order (u), stream number (Nu), and stream length (Lu). The parameters (F) reflect the texture of the drainage network, while (D) indicates the closeness of stream spacing so that these parameters are directly proportional to the degree of risk.

For relief characteristics, the main parameters are mean basin slope (Sm), relief ratio (Rr), and ruggedness number (Rn), which directly affect the degree of risk – steeper slopes producing lower filtration with more runoff and vice-versa. Based on Melton [34], Low values of ruggedness number (Rn) refer to the sub-basins are less susceptible to soil erosion; high values indicate that the sub-basins are prone to soil erosion.

For the flood risk assessment of the sub-basins in the Qena watershed, the following steps

• A number of hazard scale has been suggested for all parameters, ranging from 1 (lowest) to 5 (highest);

• The maximum and minimum values have been identified across all parameters for the sub-basins of the watershed;

• The actual degree of hazard for the sub-basins can then be calculated (with values between the minimum and maximum) from the relationship [40].

If the relationship between the parameter and the hazard degree have a directly proportional:

$$\text{Hazard degree} = \frac{4(X-Xmin)}{(Xmax-Xmin)} + 1 \qquad \text{(Eq. 1)}$$

If the relationship between the parameter and the hazard degree have an inverse proportional:

$$\text{Hazard degree} = \frac{4(X-Xmax)}{(Xmin-Xmax)} + 1 \qquad \text{(Eq. 2)}$$

where (x) is the value of the morphometric parameters, determining the hazard degree for each sub-basin. X_{min} and X_{max} are the minimum and maximum values of the parameters of all sub-basins, respectively. After using Eq. 1 and Eq. 2 for applying the ranking method to derive the hazard degree of the sub-basins based on each parameter, the method has been applied again to the sums of all parameters' hazard degrees in order to map the degrees of hazard.

Results and discussion

1) Rainfall data analysis

Comparison of the precipitation (mm d^{-1}) obtained from observed data and TRMM (averaged daily from 2012 to 2016 from the eight stations across the county) is shown in Figure 3. The patterns were well matched with each other. However, the TRMM data performance overestimated rainfall on some days and approximately equaled it on others. Comparing the daily precipitation data obtained from TRMM and rainfall from observed data shows that most rainy days are common in each of the measuring instruments.

The scatter plot in Figure 4 displays the linear relationship between the TRMM and the rain-gauge data (mm d^{-1}). Statistically, the regression procedure can be used to calibrate an unknown parameter in reference to known information. For estimation of the rainfall from the TRMM, the regression equation is:

$$RF_{TRMM} = m * (RF_{estimated}) + C \qquad \text{(Eq. 3)}$$

where RF_{TRMM} is the TRMM-detected rainfall, C is a constant, m is the slope, and $RF_{estimated}$ is the rainfall to be estimated as shown in Eq. 3. The TRMM and rain gauge data are averaged for the rainy days between 2012 and 2016 at the different locations across the country. One half of the data being used to generate the regression equation and the other half is used for the verification (see Figure 4). For the regression equation, m and C are 0.5551 and 0.1739, respectively, with a root mean square error (RMSE) = 0.837 mm d^{-1} and R^2 = 0.238. For verification

purposes, the second set of data is used, giving RMSE = 1.701 mm d^{-1} and R^2 = 0.601, which is considered acceptable in conditions with a lack of data. The correction equation can be used for water-related applications in Egypt where there is a lack of recorded rainfall data, and available records and reports are incomplete.

2) The annual time series of rainfall over the study area

Variation of rainfall over time and its behaviour focus on attention, with a view to developing the capability to receive potential threats in a timely fashion. To study temporal variation, corrected TRMM data is used due to the scarcity of observed data over the study area. However, Kwarteng et al. [41] used 27-year rainfall gauge data for analysis in Oman, while Gocic and Trajkovic [42] analyzed 30 years' worth of precipitation data from Serbia. Available data for the study area only covers 16 years. Corrected TRMM data is used to obtain the annual rainfall and plot the annual time series from 2001 to 2016 over the study area. The linear regression trend shows that rainfall over the watershed is following an increasing trend, as shown in SM 4. This increasing trend illustrates the need for further water-related studies in the study area.

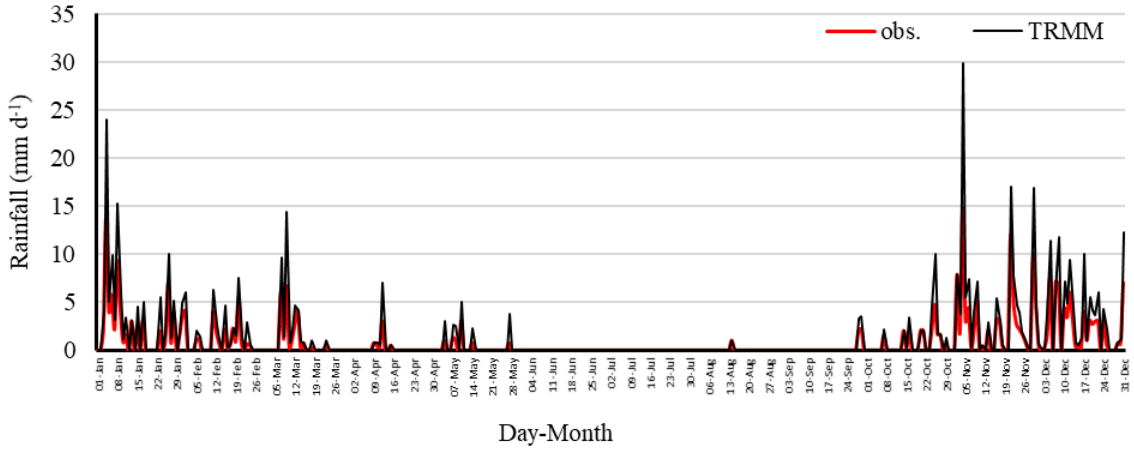

Figure 3 Day-to-day comparison of rainfall (mm d^{-1}) obtained from the TRMM and observed data.

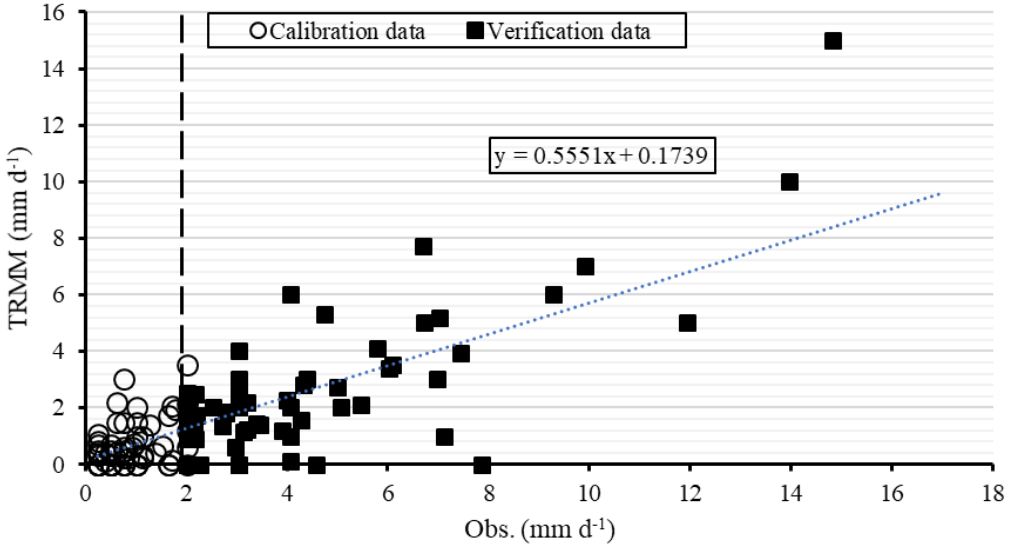

Figure 4 Scatter plot of daily rainfall averaged over 2012 to 2016 from all eight stations on rainy days.

3) Morphometric analysis

3.1) Basin geometry

The sub-basins areas from 28 km^2 to 1465 km^2 and the total area of the watershed is equal to 15488 km^2. Horton [39] classified the sub-basins by size into three categories: large (> 100 km^2), medium (50–100 km^2), and small basins (< 50 km^2). Based on Horton [39], about (84%) of the sub-basins fall into the category of large areas, while 12.51% and 3.19% of the sub-basins are in medium and small areas, respectively.

3.2) Drainage network

The characteristics assessment (using quantitative morphometric analysis of any drainage basin) provides useful information about the rocks' geological characteristics and hydrological nature of the drainage basin. Horton's law of stream numbers states that the stream number decreases linearly with an increase in stream order [39]. According to Horton's law [39], the plot of the logarithm of the number of streams, as a function of stream order, should yield a set of points lying along a straight line. Furthermore, Horton [39] states that the relation between the logarithm of cumulative stream length and stream order should follow the linear relation. Both SM 3 and 4 confirm these linear correlations, with correlation coefficients (R^2) of 0.9973 and 0.8335, respectively.

The watershed's stream order is related to the 5^{th} order and the watershed has 273 streams altogether, linked with five orders of streams. According to Smith [43], the texture ratio is divided to fine (> 16 km^{-1}), intermediate (6.4–16 km^{-1}) and coarse (< 6.4 km^{-1}). All sub-basins are in the coarse texture class, where the values of texture ratio are in the range from 0.0185 km^{-1} to 0.1096 km^{-1}. For the drainage density, [33] considered values less than 3 km^{-1} to be low drainage densities, while high drainage densities have values more than 3 km^{-1}. Drainage density values in the study area range from 0.176 km^{-1} to 4.85 km^{-1}. Sub-basins with high drainage density values indicate well-developed networks conducive to quick disposal of runoff, resulting in intense floods. Low drainage density values appear at the sub-basins characterized by low resistant and high to moderate relief terrain. The stream frequency values of the sub-basins are in the range between 0.011 km^{-2} and 0.071 km^{-2}, which according to Abboud and Nofal [44] are considered low values. These low values of stream frequency indicate that the watershed has scarce plant cover [38]. The sub-basins' stream frequencies have a small variation because of the similarity in lithology of the sub-basins. The lower drainage density values and stream frequency of the sub-basins suggest that runoff is slower and flooding is less likely to occur.

3.3) Relief characteristics

The values of the mean angle of slope are in the range from 0.9° to 12.77°, which means according to Meraj et al. [45] that the slope ranges from nearly level to a strong slope. strong slope in the eastern part of the watershed produce greater velocities and faster runoff. On the other hand, less volume of runoff and low velocities will be produced in the middle of the watershed where the slope is the nearly level slope. The sub-basins' ruggedness values range from 0.08 (which can be classified as subdued morphology) to 1.73 (morphologically extreme, including the topography of badlands). The relief ratio values are in the range from 0.561 to 4.386. Schumm [35] mentioned that the low values of relief ratio point to the presence of exposed basement rocks while higher values indicate a steep slope and high relief.

4) Flood hazard mapping

SM 5 ranks the hazard degree values for each sun-basins parameters, which can be used to assess flood hazard degree. The flood

hazard map is produced based on the general degree of hazard for all the sub-basins' parameters, applying the ranking method for summation of the hazard degrees for each sub-basin, as shown in Figure 5. The dominant feature of hazard degree is low and medium hazards. At first glance, the sub-basins characterized by a high degree of slope and large area seem to be the most hazardous, but these sub-basins are assessed as having a moderate and low hazard degree to the effect of other parameters, as analyzed in SM 5. The sub-basins with numbers 21, 31 and 55 are evaluated as being the most hazardous ones, followed by the sub-basins with numbers 12, 26, 41, 45 and 49 in the fourth hazard degree, although a small area and gentle slope characterize these sub-basins. There are 32 sub-basins with a moderate to high hazard degree (45.7% of the total number of sub-basins). Sub-basins identified as the least hazardous, represent 54.3% of the total and are concentrated in the middle of the watershed.

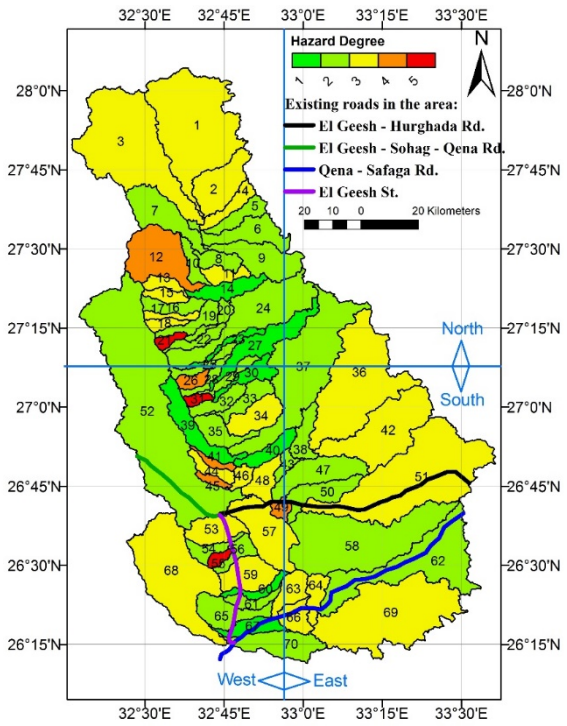

Figure 5 The flood hazard map.

5) Assessment of the monitoring system (gauge measurements)

Accurate estimation and measurement of precipitation depth and volume are also important for forecasting hazards caused by heavy rain, estimation of groundwater recharge, development of runoff models, design and operation of civil structures, and solving environmental water problems drought and flooding. Statistical analysis of the corrected TRMM data was applied to evaluate the study area's monitoring system. The average monthly rainfall from 2001 to 2016 (in SM 6) shows that rainfall over the study area is limited to the winter and spring, with spring being the wettest season and winter is the second wettest one. Almazroui [9] also concluded that spring is the wettest and winter is the second wettest season in Saudi Arabia. The rainfall frequency (see SM 7) indicates that April has been the rainiest month for five years, while January and March were the months with the highest rainfall for four years. Although January and March were repeatedly the rainiest months, it can be seen from SM 8 that rainfall during January is less than that during March, which confirms that March and April are the rainiest months overall.

Climatic data for the Wadi Qena drainage basin are traditionally acquired from the closest weather station, which is located at 26° 30′ N and 33° 06′ E. The Egyptian Meteorological Authority supposes that the weather station covers an area with a 50 km radius. To describe the distribution of precipitation over the study area, the precipitation contour map for the maximum daily rainfall in 2001, 2004, 2005, 2007, and 2014 is plotted here (as measured by TRMM) with these five years having the maximum daily rainfall between 2001 and 2016, as shown in Figure 6.

Spatial representation of the rainfall magnitude as of 3rd April 2001 and 24th March 2007 shows that the rainfall storms were beyond the station's range, as shown in Figures 7a and d,

respectively. As of 6th January 2004, and 22nd April 2005, the station was hardly covering the storms, as shown in Figures 7b and c. The catastrophic event in the study area on 9th March 2014 is well-matched with the corrected TRMM. Meanwhile, the weather station recorded no rainfall for this day, resulting in incomplete and inaccurate records for this event due to the incorrect station's position as shown in Figure 7e. Furthermore, only two sub-basins from those classified in the two highest hazard categories are within the station range. The contour maps also show the intensity of precipitation over the high-risk sub-basins beyond the station range. The current monitoring system does not adequately measure the area studied here and the northern part of the study area must be prioritized in terms of establishing new weather stations.

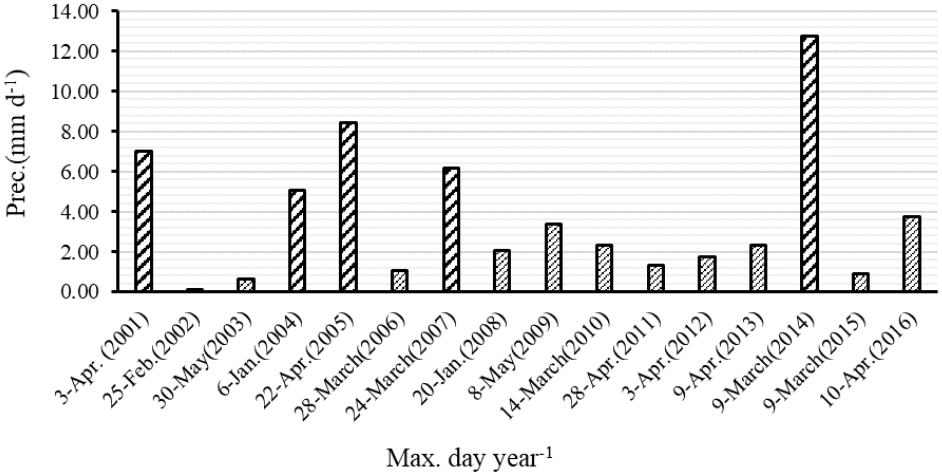

Figure 6 Maximum daily rainfall per year over the study area from 2001 to 2016.

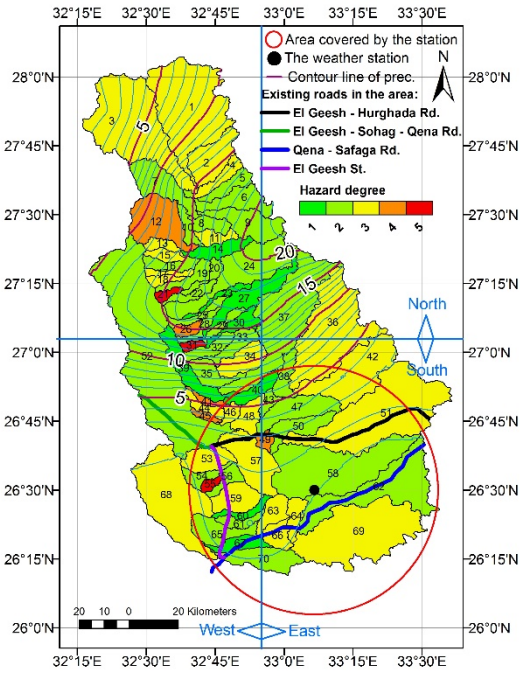

(a) Precipitation as of 3rd April 2001

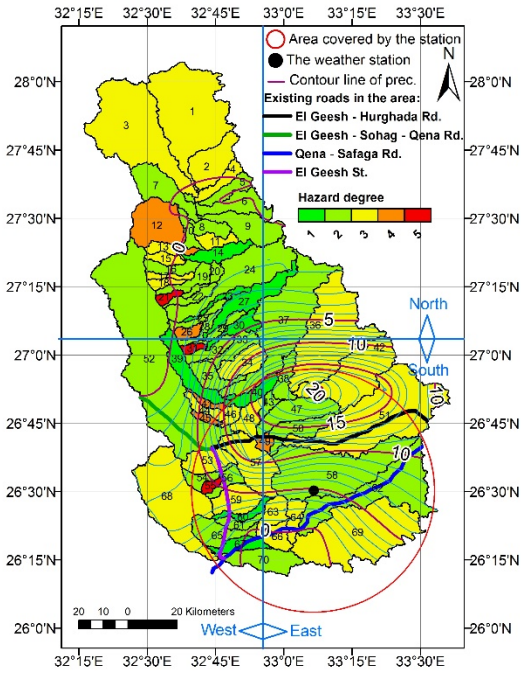

(b) Precipitation as of 6th January 2004

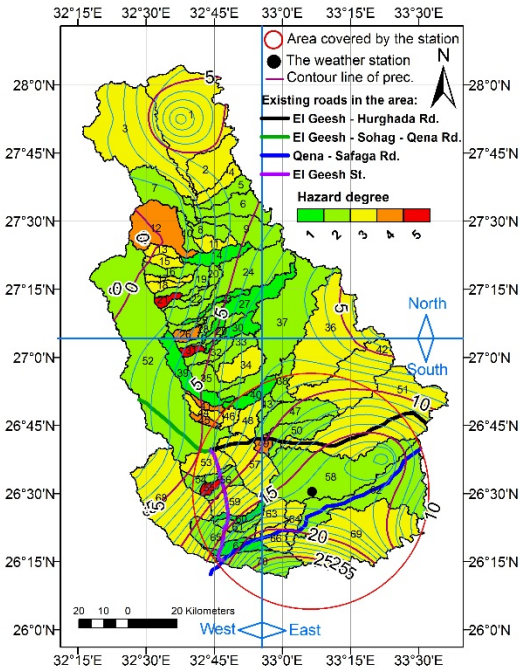

(c) Precipitation as of 22nd April 2005

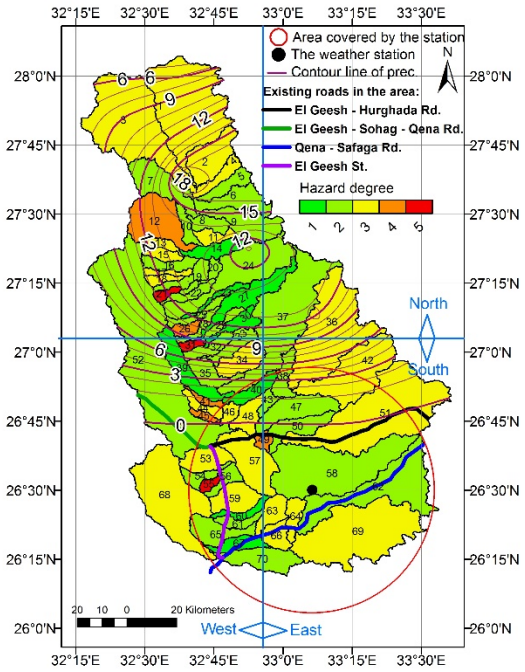

(d) Precipitation as of 24th March 2007

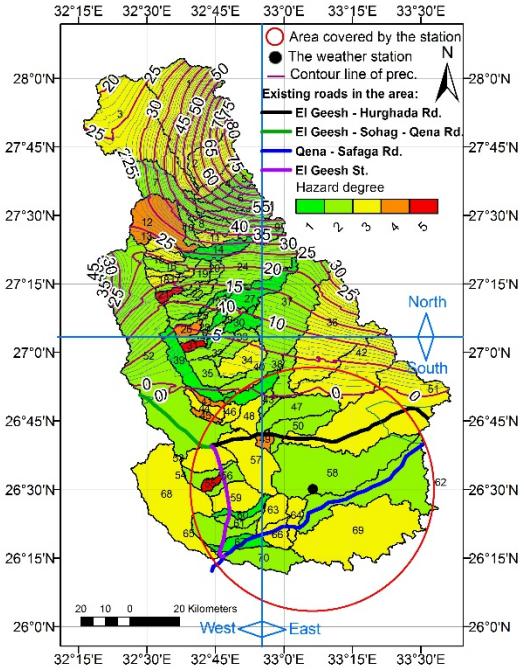

(e) Precipitation as of 9th March 2014

Figure 7 Spatial representation of rainfall magnitude over the study area as of a) 3rd April 2001; b) 6th January 2004; c) 22nd April 2005; d) 24th March 2007; and e) 9th March 2014.

Conclusion

The study tested TRMM data and recorded rainfall data from eight stations across Egypt between 2012 and 2016. Although, the TRMM data's performance overestimated the rainfall on some days and approximately equaled it on others, TRMM rainfall and observed data trends show that the patterns are well matched with

each other. Through the calibration process, a correction equation for the TRMM data was developed, producing root mean square error (RMSE) value of 0.837 mm d^{-1} and $R^2 = 0.238$. The verification process using the developed correction equation resulting RMSE value of 1.701 mm d^{-1} and $R^2 = 0.601$, which is considered acceptable under conditions with a lack of data. The results indicate that the TRMM precipitation data (after correction) can be applied as a potential alternative to ground-gauged data which match the catastrophic event on 9th March. The morphometric analysis shows that there are 32 sub-basins with a hazard degree from moderate to high., considering only two of the most hazardous sub-basins are located within the range of the station. Conclusively, a shortcoming in the current monitoring system and the northern part of the study area should be prioritized in terms of establishing a new weather station.

References

[1] Ergünay, O. Acil Yardım Planlaması ve Afet Yönetimi, Uzman Der Dergisi,1999, 6(7), 10s. Ankara.

[2] Pombo, S., de Oliveira, R.P. Evaluation of extreme precipitation estimates from TRMM in Angola. Journal of Hydrology, 2015, 523, 663–679.

[3] Haggag, M., El-Badry, H. Mesoscale numerical study of quasi-stationary convective system over Jeddah in November 2009, 2013.

[4] Dawod, G.M., Mirza, M.N., Al-Ghamdi, K.A. GIS-based estimation of flood hazard impacts on road network in Makkah city, Saudi Arabia. Environmental Earth Sciences, 2012, 67(8), 2205–2215.

[5] Hapuarachchi, H.A.P., Wang, Q.J., Pagano, T.C. A review of advances in flash flood forecasting, Hydrological Processes, 2011, 25(18), 2771–2784.

[6] Asante, K.O., Macuacua, R.D., Artan, G. A.R., Lietzow, W., Verdin, J.P. Developing a flood monitoring system from remotely sensed data for the Limpopo basin, IEEE Trans. Geoscience and Remote Sensing, 2007, 45(6), 1709–1714.

[7] Hossain, F. Towards formulation of a space-borne system for early warning of floods: Can cost-effectiveness outweigh prediction uncertainty?. Natural Hazards, 2006, 37(3), 263–276.

[8] Borga, M., Stoffel, M., Marchi, L., Marra, F., Jakob, M. Hydrogeomorphic response to extreme rainfall in headwater systems: flash floods and debris flows. Journal of Hydrology, 2014, 518, 194–205.

[9] Almazroui, M. Calibration of TRMM rainfall climatology over Saudi Arabia during 1998–2009. Atmospheric Research, 2011, 99(3–4), 400–414.

[10] Kheimi, M.M., Gutub, S. Assessment of remotely sensed precipitation products across the Saudi Arabia region. In 6th International conference on water resources and arid environments, 2014, 1617.

[11] Tekeli, A.E., Fouli, H. Evaluation of TRMM satellite-based precipitation indexes for flood forecasting over Riyadh City, Saudi Arabia. Journal of Hydrology, 2016, 541, 471–479.

[12] Saleh, A.S. Flash floods in deserts. A geomorphic study desert Wadis. Institute of Arab Research, Cairo, Egypt, 1989, 51, 1–93.

[13] El Shamy, I.Z. Recent recharge and flash flooding opportunities in the Eastern Desert, Egypt, 1992.

[14] Bajabaa, S., Masoud, M., Al-Amri, N. Flash flood hazard mapping based on quantitative hydrology, geomorphology and GIS techniques (Case study of Wadi Al Lith, Saudi Arabia). Arabian Journal of Geosciences, 2014, 7(6), 2469–2481.

[15] Singh, P., Thakur, J.K., Singh, U.C. Morphometric analysis of Morar River Basin, Madhya Pradesh, India, using remote sensing and GIS techniques. Environmental Earth Sciences, 2013, 68(7), 1967–1977.

[16] Keskin, I., Yılmaz, I. Morphometric and geological features of karstic depressions in gypsum (Sivas, Turkey). Environmental Earth Sciences, 2016, 75(12), 1040.

[17] Sanyal, J., Lu, X.X. Application of remote sensing in flood management with special reference to monsoon Asia: A review. Natural Hazards, 2004, 33(2), 283–301.

[18] Zerger, A. Examining GIS decision utility for natural hazard risk modelling. Environmental Modelling & Software, 2002, 17(3), 287–294.

[19] Sharma, S.K., Rajput, G.S., Tignath, S., Pandey, R.P. Morphometric analysis and prioritization of a watershed using GIS. Journal of Indian Water Resources Society, 2010, 30(2), 33–39.

[20] Zope, P.E., Eldho, T.I., Jothiprakash, V. Impacts of land use–land cover change and urbanization on flooding: A case study of Oshiwara River Basin in Mumbai, India. Catena, 2016, 145, 142–154.

[21] Youssef, A.M., Pradhan, B., Hassan, A.M. Flash flood risk estimation along the St. Katherine road, southern Sinai, Egypt using GIS based morphometry and satellite imagery. Environmental Earth Sciences, 2011, 62(3), 611–623.

[22] Elewa, H.H., Ramadan, E.-S.M., Nosair, A.M. Spatial-based hydro-morphometric watershed modeling for the assessment of flooding potentialities. Environmental Earth Sciences, 2016, 75(10), 927.

[23] Moawad, M.B., Abdel Aziz, A.O., Mamtimin, B. Flash floods in the Sahara: a case study for the 28 January 2013 flood in Qena, Egypt. Geomatics, Natural Hazards and Risk, 2016, 7(1), 215–236.

[24] Elsadek, W.M., Ibrahim, M.G., Mahmod, W.E., Kanae, S. Developing an overall assessment map for flood hazard on large area watershed using multi-method approach: Case study of Wadi Qena watershed, Egypt. Natural Hazards, 2019, 95(3), 739–767.

[25] Elsadek, W.M., Ibrahim, M.G., Mahmod, W.E. Runoff hazard analysis of Wadi Qena Watershed, Egypt based on GIS and remote sensing approach. Alexandria Engineering Journal, 2019, 58(1), 377–385.

[26] Elsadek, W.M., Ibrahim, M.G., Mahmod, W.E. Flash flood risk estimation of Wadi Qena Watershed, Egypt using GIS based morphometric analysis. Applied Environmental Research, 2018, 41(1), 41–50.

[27] Geiger, R. Klassifikation der klimate nach W. Köppen. Landolt-Börnstein–Zahlenwerte und Funktionen aus Phys. Chemie, Astron. Geophys. und Tech., 1954, 3, 603–607.

[28] Bandel, K., Kuss, J., Malchus, N. The sediments of Wadi Qena (eastern desert, Egypt). Journal of African Earth Sciences, 1987, 6(4), 427–455.

[29] Brown, J.E.M. An analysis of the performance of hybrid infrared and microwave satellite precipitation algorithms over India and adjacent regions. Remote Sensing of Environment, 2006, 101(1), 63–81.

[30] Prudhomme, C., Reed, D.W. Mapping extreme rainfall in a mountainous region using geostatistical techniques: A case study in Scotland. International Journal of Climatology, 1999, 19(12), 1337–1356.

[31] Patel, D.P., Gajjar, C.A., Srivastava, P.K. Prioritization of Malesari mini-watersheds through morphometric analysis: a remote sensing and GIS perspective. Environmental Earth Sciences, 2013, 69 (8), 2643–2656.

[32] Vittala, S.S., Govindaiah, S., Gowda, H.H. Morphometric analysis of sub-watersheds in the Pavagada area of Tumkur district, South India using remote sensing and GIS techniques. Journal of the Indian Society of Remote Sensing, 2004, 32(4), 351.

[33] Horton, R.E. Erosional development of streams and their drainage basins; hydro-physical approach to quantitative morphology. Geological Society of America Bulletin, 1945, 56(3), 275–370.

[34] Melton, M.A. An analysis of the relations among elements of climate, surface properties, and geomorphology. Columbia University New York, 1957.

[35] Schumm, S.A. Evolution of drainage systems and slopes in badlands at Perth Amboy, New Jersey. Geological Society of America Bulletin, 1956, 67(5), 597–646.

[36] Haggett, P. Locational analysis in human geography, 1966.

[37] Strahler, A.N. Quantitative analysis of watershed geomorphology. Eos Transactions American Geophysical Union, 1957, 38 (6), 913–920.

[38] Strahler, A.N. Part II. Quantitative geomorphology of drainage basins and channel networks. Handbook of Applied Hydrology. McGraw-Hill, New York, 1964, 4–39.

[39] Horton, R.E. Drainage-basin characteristics. Eos Transactions American Geophysical Union, 1932, 13(1), 350–36.

[40] Davis, J.C. Statistics and data analysis in geology. Wiley, New York, 1973.

[41] Kwarteng, A.Y., Dorvlo, A.S., Vijaya Kumar, G.T. Analysis of a 27-year rainfall data (1977–2003) in the Sultanate of Oman. International Journal of Climatology, 2009, 29(4), 605–617.

[42] Gocic, M., Trajkovic, S. Analysis of changes in meteorological variables using Mann-Kendall and Sen's slope estimator statistical tests in Serbia. Global and Planetary Change, 2013, 100, 172–182.

[43] Smith, K.G. Erosional processes and landforms in badlands national monument, South Dakota. Geological Society of America Bulletin, 1958, 69(8), 975–1008.

[44] Abboud, I.A., Nofal, R.A. Morphometric analysis of wadi Khumal basin, western coast of Saudi Arabia, using remote sensing and GIS techniques. Journal of African Earth Sciences, 2017, 126, 58–74.

[45] Meraj, G., Romshoo, S.A., Yousuf, A.R., Altaf, S., Altaf, F. Assessing the influence of watershed characteristics on the flood vulnerability of Jhelum basin in Kashmir Himalaya. Natural Hazards, 2015, 77(1), 153–175.